Figure S1, related to Figure2

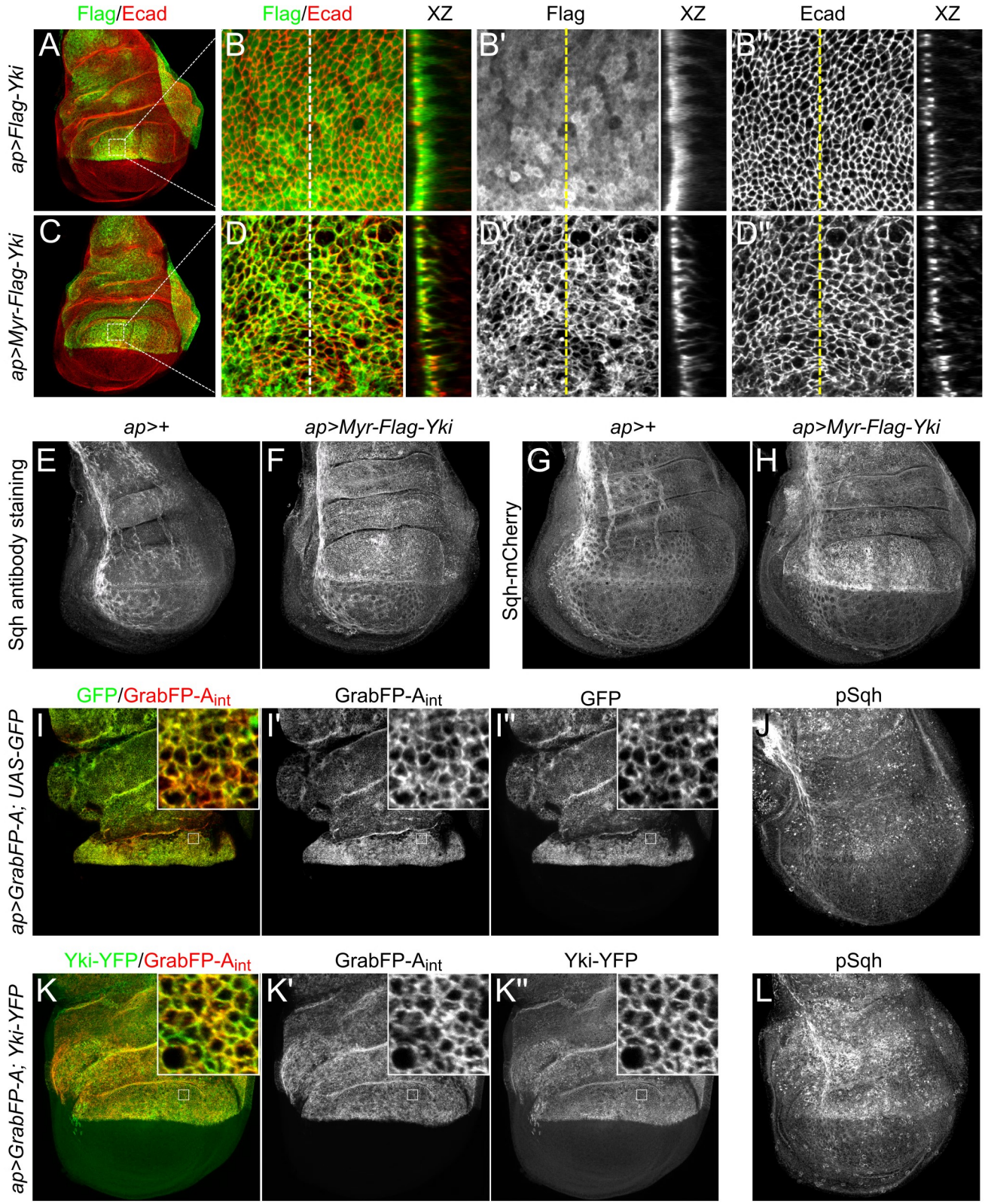

Figure S1, related to Figure 2. Cortical Yki promotes activation of myosin

(A-D) *Myr-yki* expressed in the wing epithelium is tightly membrane-associated and enriched at the AJR.

Flag-tagged wild-type *Yki* and *Myr-Yki* were ectopically expressed in the dorsal compartment of wing discs and stained with anti-Flag and anti-Ecad (A, C). Ecad staining was used to mark AJs. Boxes in A, C) indicate area of wing disc shown in (B-B'' and D-D''). Wild-type Yki appeared mostly cytoplasmic whereas Myr-Yki is enriched cortically. XZ planes show cross-section views as marked by the dashed lines.

(E-H) Membrane-associated Yki promotes cortical accumulation of myosin.

Anti-Sqh staining and a *sqh:mCherry* reporter were used to assay Sqh levels in cells expressing *Myr-Yki.* Myr-Yki caused a noticeable increase in anti-Sqh staining and Sqh-mCherry fluorescence, indicating increased myosin accumulation at the cell cortex.

(I-L) Endogenously expressed Yki-YFP anchored at the cortex promotes myosin activation. GrabFP-A_{int} was used to target GFP (I-I'') or Yki-YFP (K-K'') to the AJR. Targeted Yki-YFP (L), but not GFP (J), caused increased pSqh staining.

Figure S2, related to Figure3

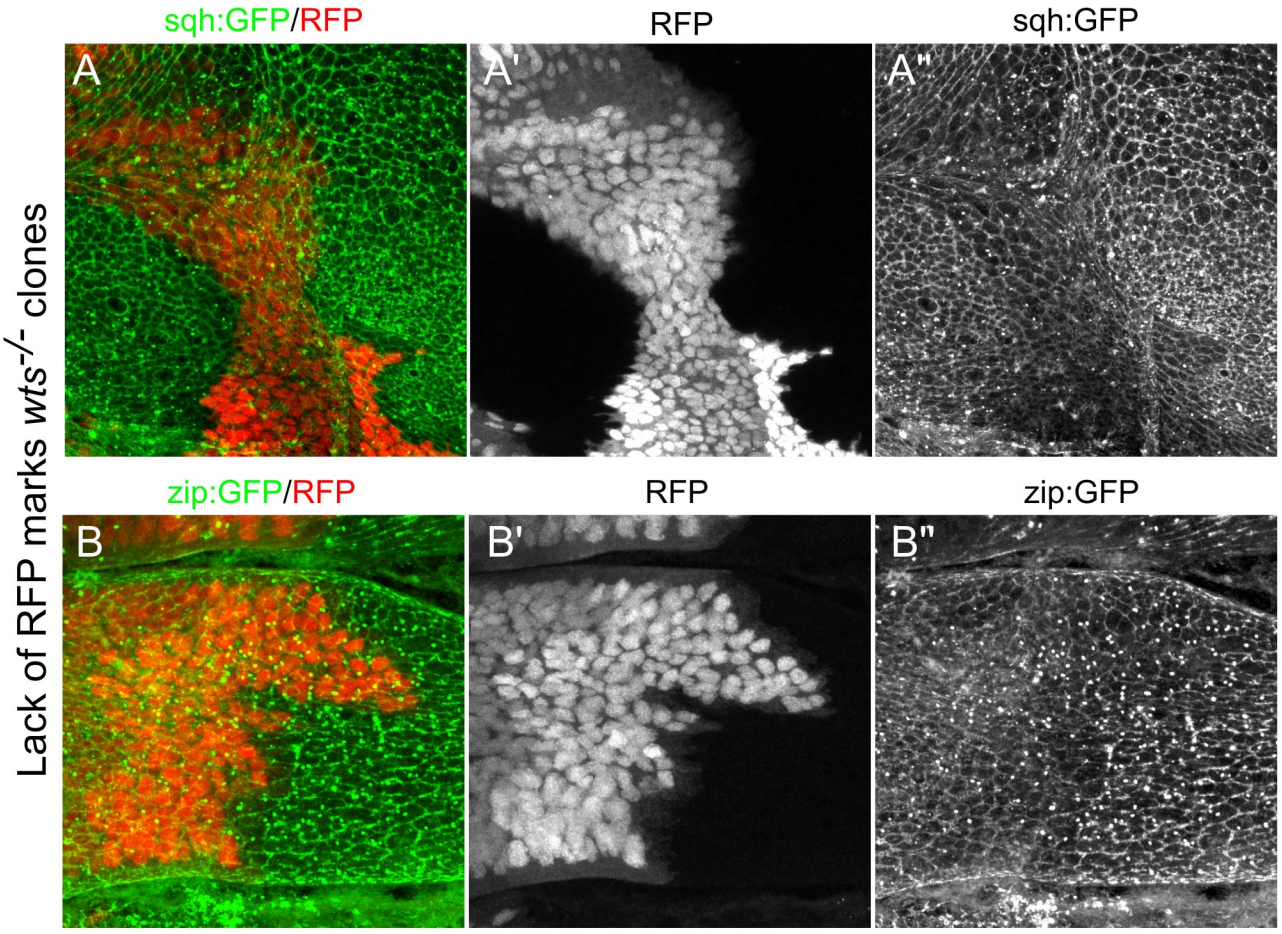

Figure S2, related to Figure 3. Hippo pathway inactivation causes myosin activation

Sqh:GFP and Zip:GFP reporters were used to assay myosin levels in *wts* clones. Lack of RFP marks *wts* null (wts^{X1}) clones. Loss of *wts* caused increased Sqh:GFP (A) and Zip:GFP (B) levels, consistent with increased myosin activation.

Figure S3, related to Figure 4

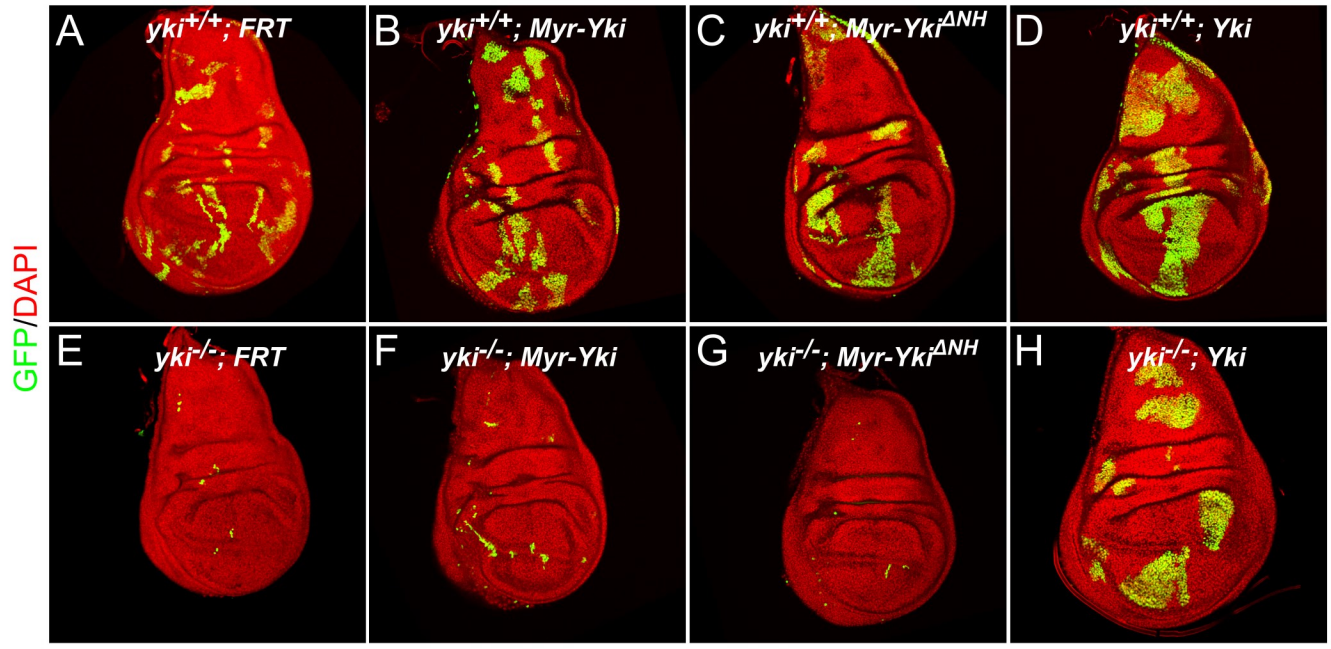

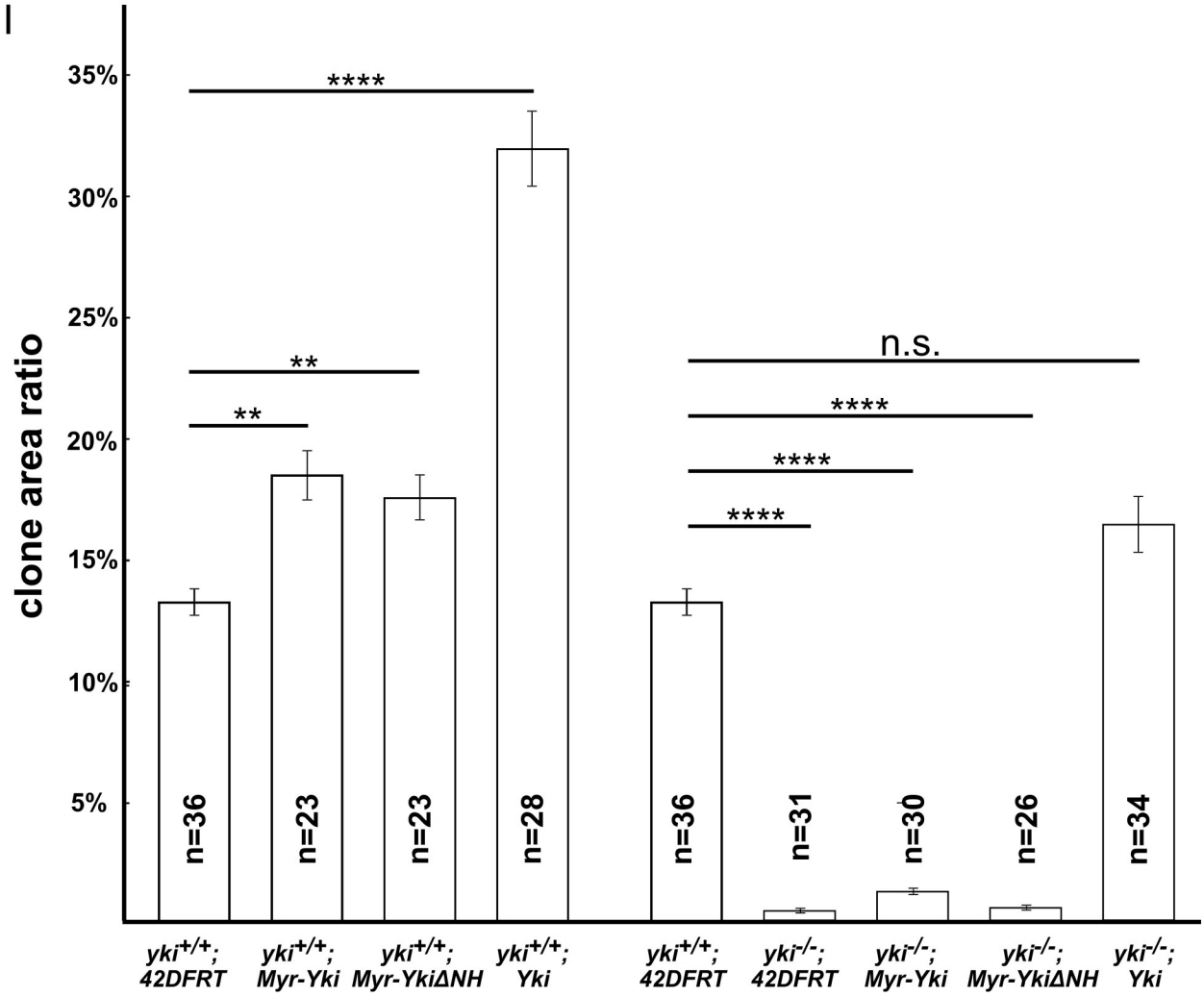

Figure S3, related to Figure 4. Cortical Yki promotes growth via endogenous Yki

(A-H) MARCM clones that expressed *Myr-Yki, Myr-Yki$^{\Delta NH}$, or* wild-type *Yki* in the background of wild-type *yki* (A-D) or a *yki* null mutation (*yki^{B5}*) (E-H) were generated. All three transgenes caused overgrowth in the background of wild-type *yki. yki* null clones displayed undergrowth as expected. Only wild-type *Yki* rescued the undergrowth of *yki* null clones - neither *Myr-Yki* nor *Myr-Yki$^{\Delta NH}$* rescued these clones.

(I) Quantification of growth of mosaic clones of the indicated genotypes. Clone area ratio was obtained by dividing area of all GFP marked clones by the area of the entire disc. Data are represented as mean ± SEM. Asterisks represent statistical significance of the difference between selected groups (**** $p < 0.0001$, *** $p < 0.001$, ** $p<0.01$, n.s. [not significant, $p>0.05$], One-way ANOVA and Games-Howell test, n = number of wing discs).

Figure S4, related to Figure 4

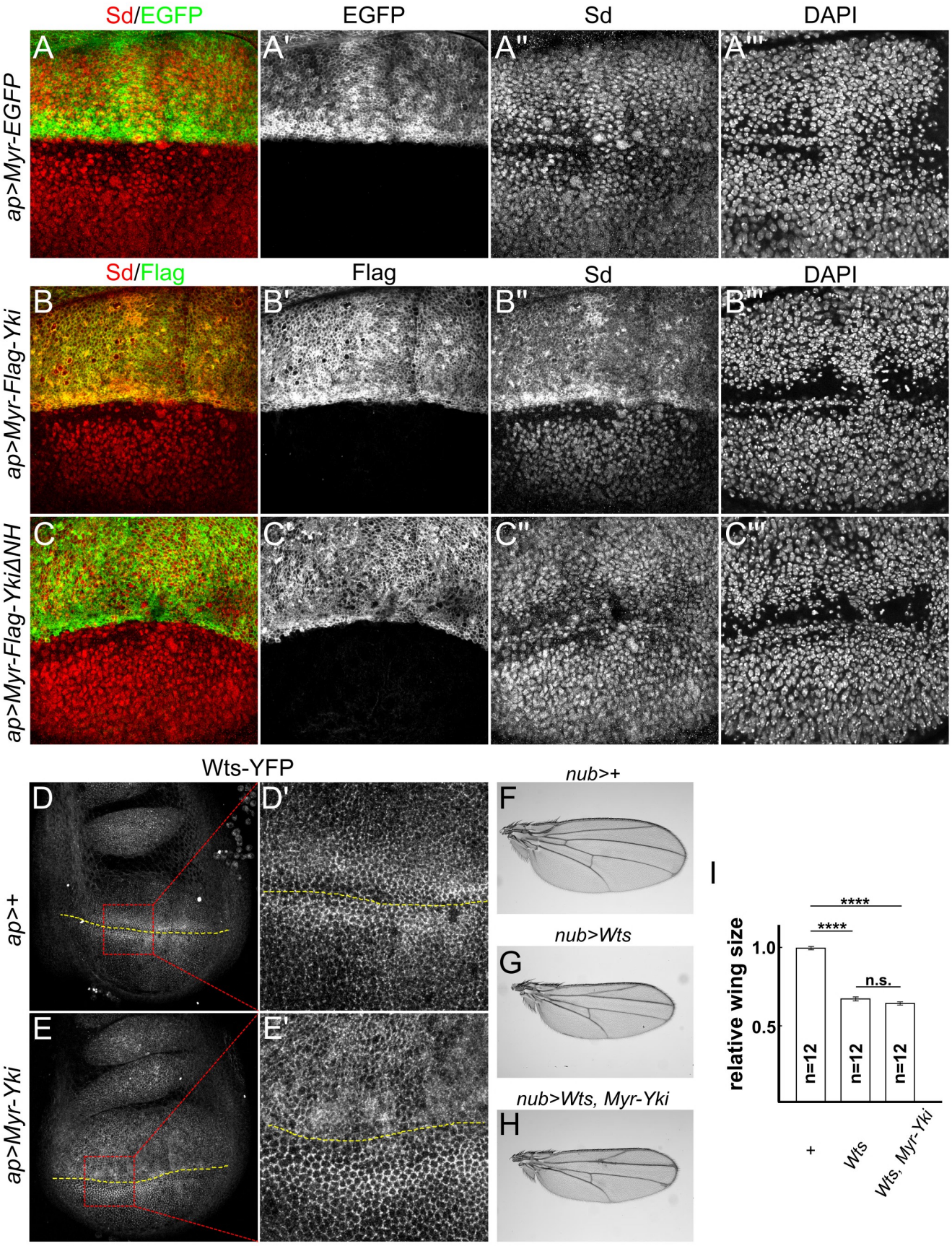

Figure S4, related to Figure 4. Myr-Yki recruits Sd, but not Wts to the AJR

(A-C''') *Myr-EGFP* (control) and Flag-tagged *Myr-Yki* and *Myr-Yki*$^{\Delta NH}$ were ectopically expressed in the dorsal compartment of wing imaginal discs. Anti-flag staining was used to visualize Myr-Yki and Myr-Yki$^{\Delta NH}$ localization. DAPI was used to show nuclei. Anti-Sd staining showed nuclear localization in cells expressing *Myr-EGFP* (A'') and *Myr-Yki*$^{\Delta NH}$ (C''). In contrast, in cells expressing *Myr-Yki,* Sd co-localized with Myr-Yki at the cell cortex (B'').

(D-E') Myr-Yki does not sequester Wts at the AJR. Endogenously expressed Wts-YFP was examined with (D-D') or without Myr-Yki (E-E') expression. Myr-Yki expression did not cause increased cortical accumulation of Wts-YFP (E-E'). Red boxes denote regions shown in higher magnification insets (D',E'). The boundary of expression is marked with a dotted yellow line.

(F-I) Myr-Yki does not suppress Wts induced undergrowth. Representative images of female adult wings of indicated genotypes are shown (cultured at 18 °C). Ectopic expression of Wts in the wing caused strong undergrowth (G) compared with control (F). Myr-Yki expression did not suppress Wts induced undergrowth (H). (I) Quantification of wing sizes for the indicated genotypes. Data are represented as mean ± SEM. Asterisks represent statistical significance of the difference between selected groups (**** $p<0.0001$; n.s.: not significant [$p > 0.05$], One-way ANOVA and Tukey's HSD test, n = number of wings).

Figure S5, related to Figure 5

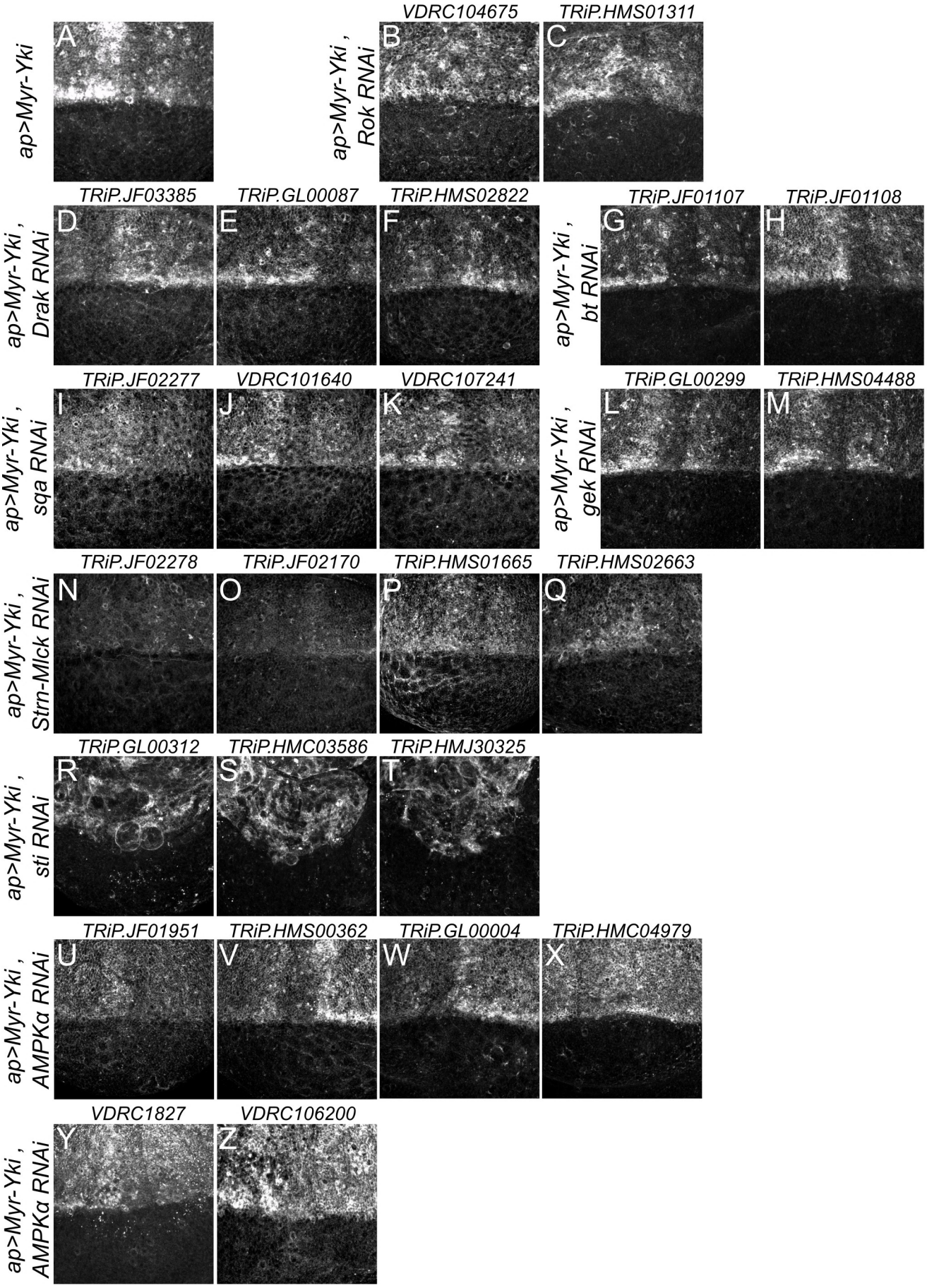

Figure S5, related to Figure 5. Yki activates Sqh via the Sqh kinase Strn-Mlck

(A-C) Yki does not activate myosin via Rok. Two independent RNAi transgenes for Rok were used to deplete Rok in cells expressing *Myr-Yki* and stained with pSqh antibody to assay myosin activation. Neither RNAi suppressed the *Myr-Yki*-induced pSqh increase, suggesting that cortical Yki does not act through Rok to activate myosin.

(D-Z) Screening for Sqh kinases that mediate the myosin activation function of cortical Yki. To screen known or predicted *Drosophila* myosin light chain kinases to determine if they are necessary for Yki-induced Sqh activation, at least two independent RNAi transgenes for the following kinases were co-expressed in wing imaginal discs with *Myr-Yki: Death-associated protein kinase related* (*Drak*), *bent* (*bt*), *spaghetti-squash activator* (*sqa*), *genghis khan* (*gek*), *Stretchin-Mlck* (*Strn-Mlck*), *sticky* (*sti*), or *AMP-activated protein kinase α subunit* (*AMPKα*). TRiP or Vienna Drosophila Resource Center (VDRC stocks) identifiers are indicated. Two Strn-Mlck RNAi lines (TRiP.JF02278, TRiP.JF021) strongly suppressed the increased pSqh staining caused by Myr-Yki expression. One AMPKα RNAi line (TRiP.JF01951) displayed weak suppression.

Figure S6, related to Figure 5

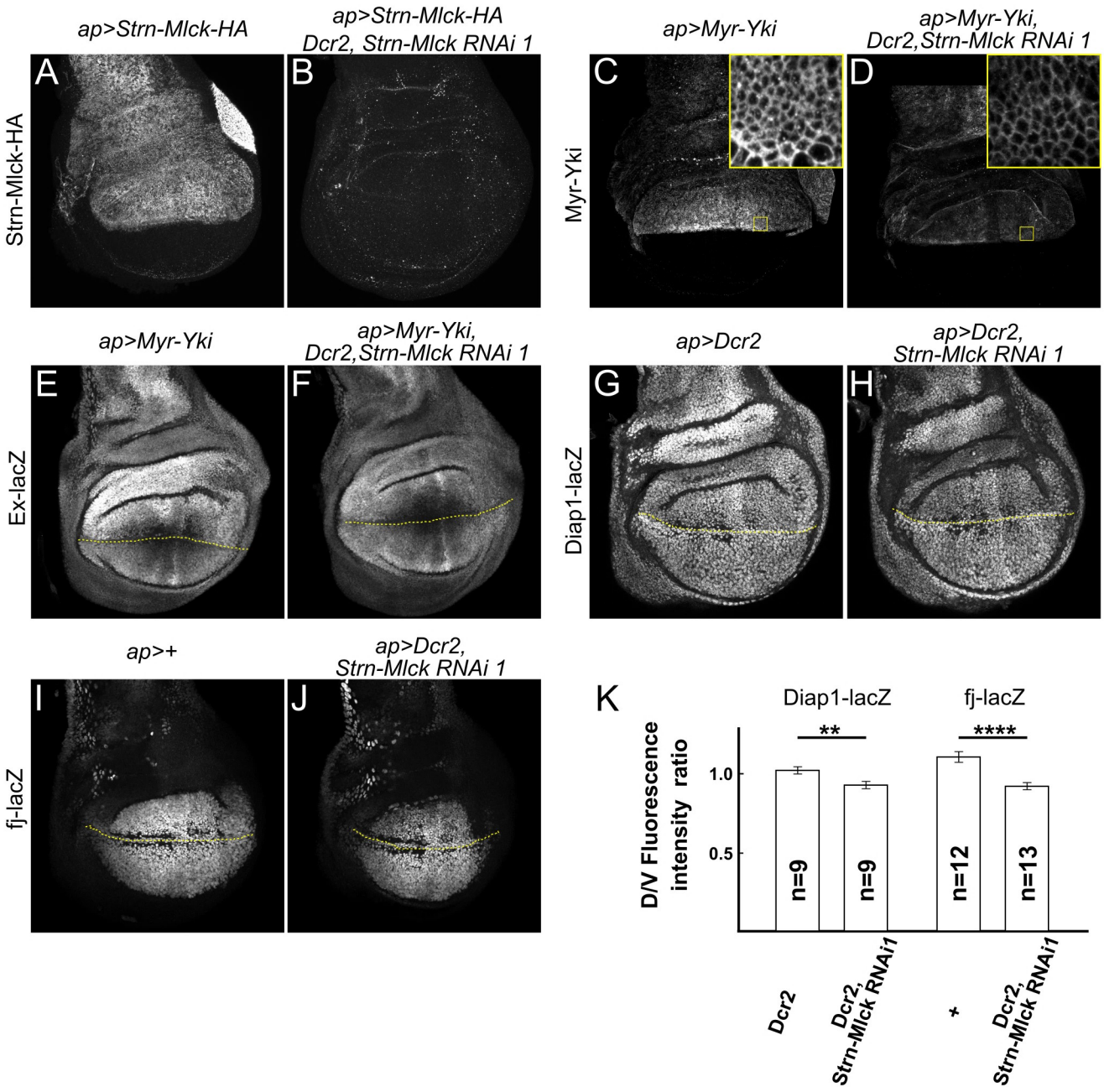

Figure S6, related to Figure 5. Strn-Mlck regulates growth via the Hippo pathway

(A-B) *Strn-Mlck RNAi 1* strongly knocked down expression of a UAS-Strn-Mlck-HA transgene, suggesting this RNAi transgene effectively depletes endogenous Strn-Mlck.

(C-D) *Strn-Mlck RNAi* does not affect subcellular localization of Myr-Yki. Yellow boxes denote regions shown in high magnification insets. Note the fluorescence intensity was lower in Strn-Mlck RNAi cells, indicating lower protein level. Samples were stained together and acquired with the same parameters.

(E-F) *Strn-Mlck RNAi* suppresses Myr-Yki-induced up-regulation of *ex-lacZ*, a reporter for Hippo pathway activity. The dotted yellow line indicates the boundary of transgene expression (expression is above the line).

(G-K) Strn-Mlck negatively regulates the Hippo pathway under normal physiological conditions. *Strn-Mlck RNAi* caused reduced expression of *Diap1-lacZ* (G-H) and *fj-lacZ* (I-J), two Hippo pathway reporters, indicating that Strn-Mlck negatively regulates the Hippo pathway. Quantification of the dorsal-ventral (D/V) ratio of Diap1-lacZ and fj-lacZ staining intensity is displayed in (K). Dotted yellow lines indicate the boundary of transgene expression. Data are represented as mean ± SEM. Asterisks represent statistical significance of the difference between selected groups (** $p<0.01$, **** $p<0.0001$. One-way ANOVA and Tukey's HSD test, n = number of wing discs).

Figure S7, related to Figure 7

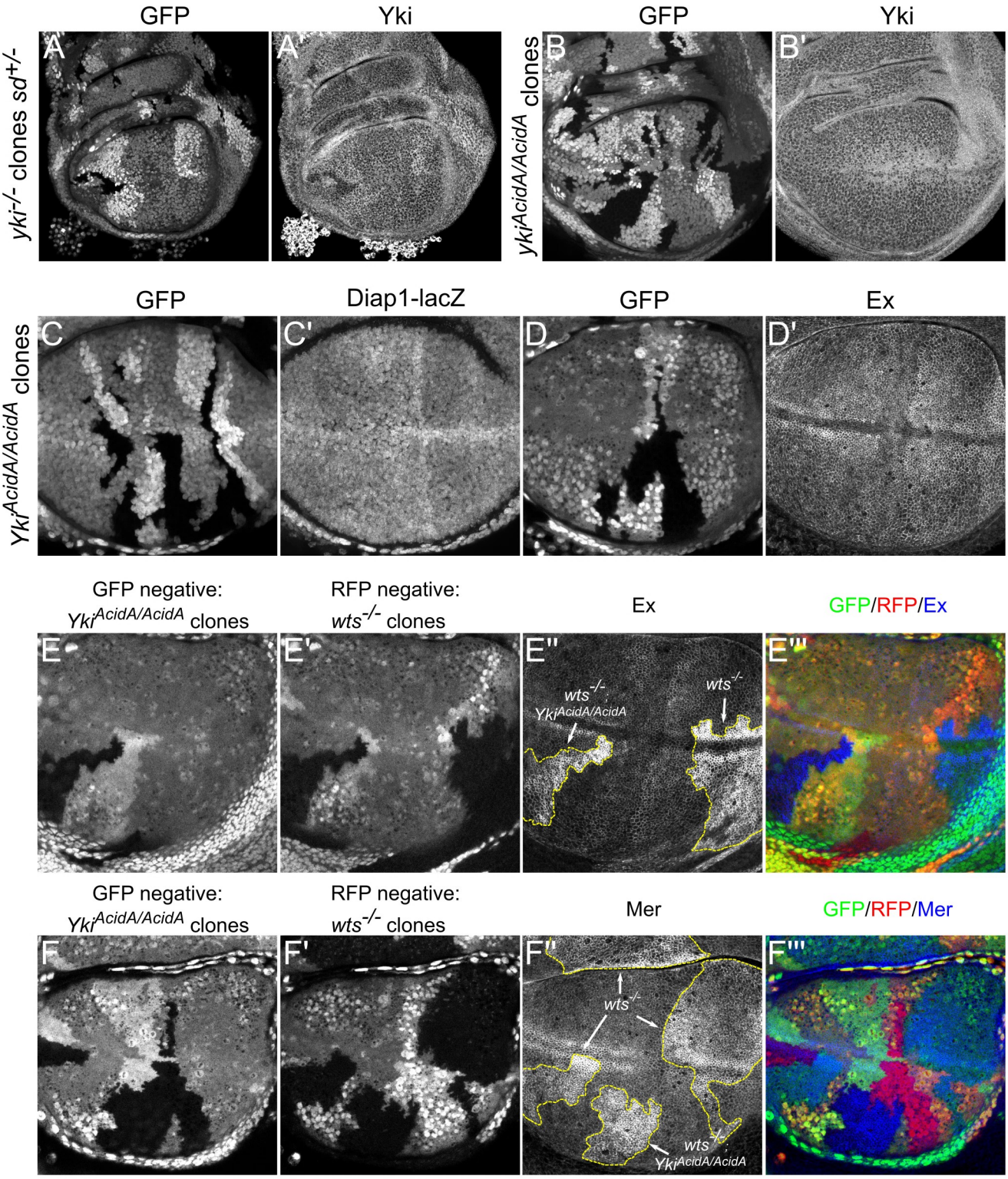

Figure S7, related to Figure 7. The *yki*^{AcidA} mutation affects Yki's myosin activation function but not its transcriptional function

(A-B') The *yki*^{AcidA} mutation does not affect *yki* expression level. *yki* null (*yki*^{B5}) clones were generated in a *sd* heterozygous background (*sd*$^{47M/+}$) because cells lacking Yki survive better when dosage of *sd*, which on its own represses target gene expression (Koontz et al., 2013), is decreased. Despite some background staining, anti-Yki staining is clearly reduced in *yki* null clones. Also note that Yki staining is noticeably increased in sister clones in which there are two copies of wild-type *yki*. In contrast, anti-Yki staining was not affected in *yki*$^{AcidA/AcidA}$ clones or sister clones relative to surrounding *yki*$^{AcidA/+}$ cells, indicating that Yki expression level is not affected by the mutation.

(C-D') The *yki*^{AcidA} mutation does not affect *yki* target gene expression under normal physiological conditions. Expression of the *Diap1-lacZ* transcriptional reporter and anti-Ex staining are not altered in *yki*$^{AcidA/AcidA}$ clones, suggesting the *yki*^{AcidA} mutation does not detectably reduce *yki* target gene expression.

(E-F''') The *yki*^{AcidA} mutation is able to fully activate *yki* target gene expression in response to Hippo pathway inactivation. To test if the *yki*^{AcidA} mutation affects Yki transcriptional function under conditions where it should be maximally transcriptionally active, expression of the Yki targets Mer and Ex was compared between *wts*$^{-/-}$ (*wts*$^{X1/X1}$) clones and *wts*$^{-/-}$*; yki*$^{AcidA/AcidA}$ double clones. In both types of clones, expression of Mer and Ex are dramatically increased in a similar fashion, suggesting that *yki*^{AcidA} mutation does not affect Yki's transcriptional activity. Dashed yellow lines mark clone boundaries.

Supplemental Table 1, related to Figures 2, 6, and 7. Mean Dorsal/Ventral (D/V) pSqh Fluorescence Intensity Ratio

Genotype	Mean D/V pSqh ratio	SEM	Sample size	p
apGal4>+	1.10	0.02	9	NA
apGal4>Myr-Yki (Random insertion)	2.82	0.09	10	<0.0001
apGal4>Myr-Yki (86Fb integration)	3.84	0.23	10	<0.0001
apGal4>Myr-Yki^{AcidA} (86Fb integration)	1.32	0.03	10	0.0001
apGal4>Myr-Yki$^{1-34}$-GFP (86Fb integration)	1.65	0.02	10	<0.0001
apGal4>Yki (Random insertion)	1.22	0.02	10	0.005
apGal4>GrabFP-A$_{int}$, UAS-GFP	1.16	0.02	11	NA
apGal4>GrabFP-A$_{int}$, Yki-YFP	1.38	0.03	10	<0.0001

Sqh activation quantified as the ratio of pSqh fluorescence intensity between D/V compartments. p value is calculated using One-Way ANOVA and Games-Howell post-hoc test. Different Yki transgenes were compared with control. GrabFP-A_{int}, Yki-YFP was compared with GrabFP-A_{int}, UAS-GFP. SEM: Standard Error of Mean.